Chapter

Treatment Analysis of Welding Structure in the Presence of a Crack Type Defects

Mersida Manjgo and Meri Burzic

Abstract

The largest number of welded structures in operating conditions is exposed to variable loads, which is why the share of fatigue fracture in the failure of welded structures is higher than others. The essence of construction with fracture safety is that the structure can withstand the designed load in the designed time. If a crack is detected during operation, it is possible to predict the development of damage during the service life as well as the load-bearing capacity of the structure depending on the development of damage. The paper describes a new system for monitoring fatigue crack growth, which is based on the change in the resistance of the measuring foil during crack growth. The system is compatible with the basic settings of the ASTM E647–86 standard, which refers to the determination of the fatigue crack growth rate.

Keywords: welded joint, fatigue crack, fatigue threshold, crack growth rate

1. Introduction

Mass application of welded structures began with the development of welding procedures on the one hand and the development of steels with suitable properties on the other. Along with welding processes, in parallel, methods for assessing the safety of welded joints were also developed.

Construction materials and welded joints can contain defects and microcracks that are the beginnings of fractures. Exploitation conditions can lead to cracking even if there are no defects in the material, e.g., at places of stress concentration caused by the design of the structure. Under the influence of unfavorable exploitation factors, such as fatigue and corrosion, cracks can grow steadily, and after enough time, reach a critical size and cause breakage.

Fatigue is the phenomenon of gradual destruction of a material due to the long-term action of a periodically changing load. Damage to structures, caused by material fatigue, represents 50 ÷ 90% of all damage to structures in exploitation [1]. The significance of fatigue damage is obvious because a large number of such damages lead to catastrophic fractures.

The traditional, well-known, S-N approach is based on the experimental determination of the dependence of the stress amplitude from the number of cycles to fracture.

This standard method is built into many standards and regulations and is widely used in the design of welded and other structures. In this test, as a rule, only the number of changes of the load to fracture under the action of a constant range load

is determined, and the standard only requires information on the magnitude of the stress at which crack and fracture initiation does not occur after a certain number of cycles (usually between 10^6 and 10^8 cycles).

In the presence of cracks, the question arises of its development under the action of a variable load.

Fatigue crack growth is a very complex process that depends on a number of variables [2]:

- the intensity of the effective stress field at the crack tip defined by the K-factor;
- type and form of load;
- environment (aggressiveness, temperature, humidity),
- mechanical and metallurgical characteristics of the material

The method of fracture mechanics is based on linearly elastic fracture mechanics and originates from the Paris' law of 1962, and is still applied, although the impact of large plastic deformations around the crack tip has not been fully taken into account. The constants that occur such as "C" i "m" in Paris' law $da/dN=C\ \Delta K^m$, must be determined separately for each material and the specific test conditions. These data are essential for three types of fatigue analysis:

- to accurately determine fatigue crack behavior
- to estimate the life of the structure
- to calculate fatigue damage

2. Determination of dynamic characteristics of welded joint

Metal fatigue is defined as the process of cumulative damage under the action of variable load, which is manifested by the appearance of fatigue cracks and fractures. The fatigue strength of welded joints is determined by testing the specimens at variable load until a crack or fracture occurs.

The test was performed on a high-frequency AMSLER pulsator. The high-frequency pulsator can achieve a sinusoidal alternating load in the range from −100 kN to +100 kN. In order to more fully assess the behavior of the material under the action of variable load, and having in mind the dimensions of the specimen, the most critical case of the action of variable load was made, namely alternating variable load tension - pressure (R = −1), **Figure 1**.

It is clear that the strength at high cyclic fatigue depends on the properties of the constituents of the welded joint. Therefore, data are needed for BM and WM, but also for HAZ, which makes testing of welded joints in high-cyclic fatigue complex and expensive. The aim of the test is to determine the points in the S-N diagram (construction of the Wehler curve) and to determine the permanent dynamic strength S_f. The test procedure as well as the specimen are defined according to ASTM E466 [3]. The appearance of the test tube with variable load is shown in **Figure 2**.

The determination of the maximum dynamic stress at which no crack-type error is initiated in smooth construction forms is shown graphically in the form of Weller curves (S-N diagrams) in **Figure 3**. for butt-welded joint specimen and **Figure 4** for specimen removed from BM.

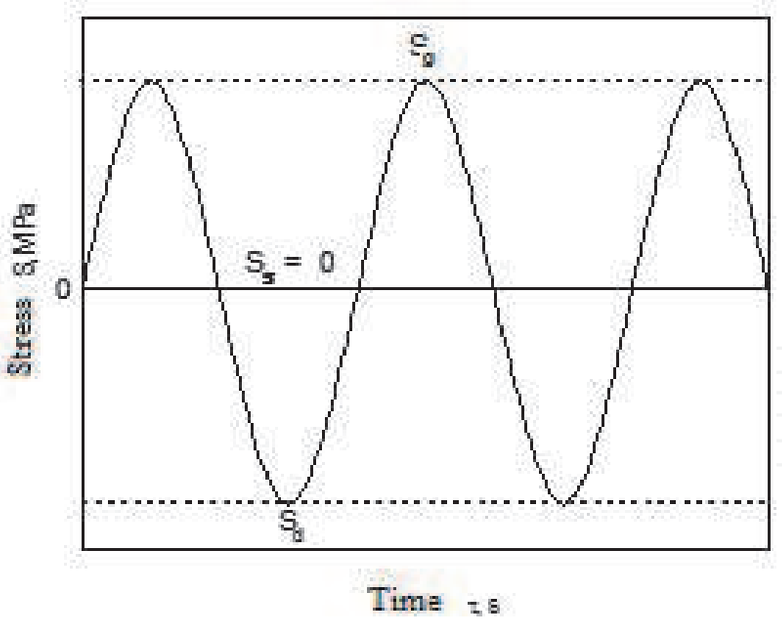

Figure 1.
Alternating load scheme. R = −1.

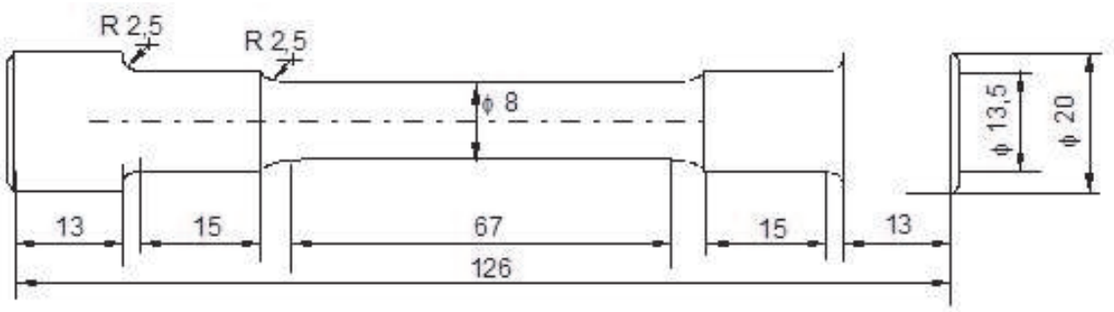

Figure 2.
Dynamic specimen according to ASTM E466.

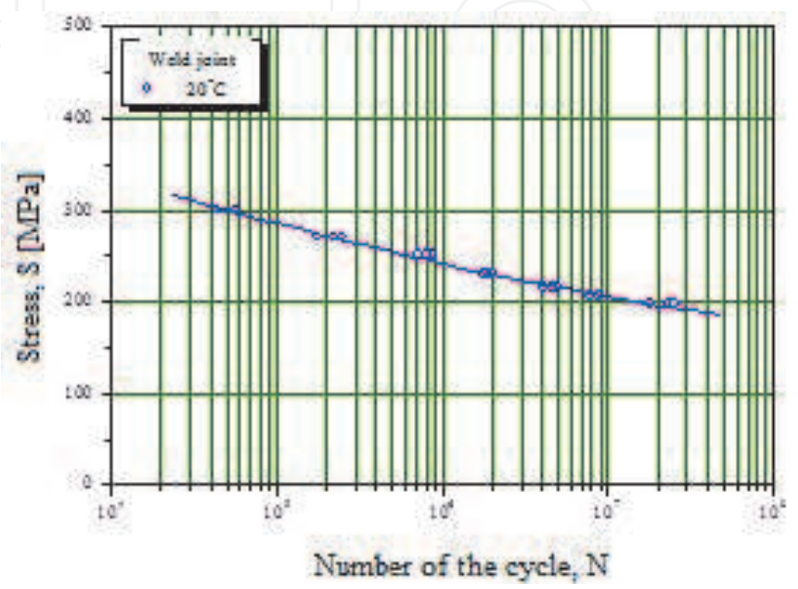

Figure 3.
S-N diagram of speciemn taken out of butt welded joint and tested at room temperature.

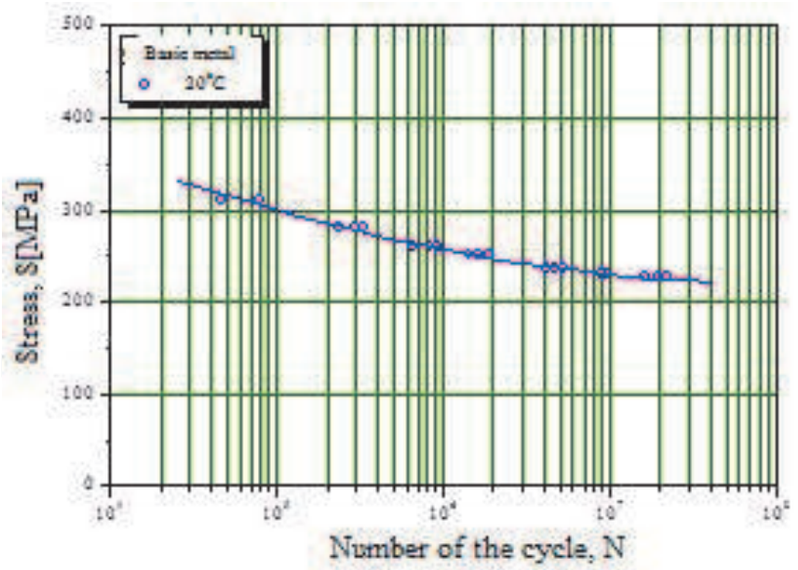

Figure 4.
S-N diagram of speciemn extracted from the new BM and tested at room and operating temperatures.

To construct one Weller curve and determine the permanent dynamic strength, it is necessary to test the specimen at 6 to 7 different load levels. According to the ASTM E 466 standard, three specimen were tested for each load level, which is a total of 21 specimen. Therefore, this test is extremely expensive and justified when design data are required, primarily from the aspect of fatigue and fracture mechanics. So when designing parts exposed to long-term variable load in the total design life of the structure.

The traditional, well-known, S-N approach is based on the experimental determination of the dependence of the stress amplitude from the number of cycles to fracture.

3. Fatigue analysis from fracture mechanics angle

The origin of the fault may be related to design and construction, technology, and producing the structure, control, and testing. The continuance of construction then depends only on the possibility and conditions of crack growth from the initial failure. The essence of construction with fracture safety is that the structure can withstand the designed load in the designed time. If a crack is detected during operation, it's possible to predict the development of damage during the service life as well as the load-bearing capacity of the structure depending on the development of damage [4].

The most important characteristics for the operational safety of structures are the ones that describe the appearance and growth of cracks under the influence of variable load. A generally accepted characteristic, in this case, is fatigue strength. Accordingly, the design of structural parts based on possible material fatigue is based on the use of fatigue strength, and empirical recommendations, derived from the analysis of parts failure in operation and extensive testing [4].

The appearance of a fatigue crack requires that the behavior of the material around the crack tip is considered based on the micromechanical aspect. The initiation of cracks and their growth condition that the micromechanical aspect of the behavior of the material becomes important for the assessment of the operational safety of structural parts. The existence of a singularity in the form of a crack tip indicates the application of fracture mechanics and its parameters, such as stress

intensity factor, crack opening, and contour J-integral. Paris' crack growth law, which determines the dependence of the load and the corresponding range of stress intensity factors, with the crack growth rate per cycle, is generally accepted today [4].

3.1 Fatigue crack growth rate da/dN i ΔK_{th}: Paris' law

The need to introduce fracture mechanics into the study of fatigue behavior arose from the analysis of crack growth under cyclic loading.

Many data on fatigue crack growth were obtained by examining CT specimen, which were exposed to loads with a constant amplitude ΔP, **Figure 5** [5].

In **Figure 5** a typical form of crack length dependence on the number of load cycles *a*-N for three load range levels ΔP = const where $\Delta P_1 < \Delta P_2 < \Delta P_3$ is shown.

It is noticeable that with the increasing number of cycles N and crack length "a", the crack growth rate defined by the slope of the tangent increases steadily. Also, with the increase in the load range ΔP, there is a faster increase of the speed gradient. In other words, the crack, for example, of length a1 in **Figure 1**, grows faster at the load amplitude ΔP_3 than at the load ΔP_2 or ΔP_1.

Numerous theoretically and empirically defined dependencies in the form $da/dN = f(P, a)$ can be found in the literature, which emphasizes the importance of load and cracks length. The first to define the range of stress intensity factor $\Delta K = f(\sigma, a)$ in the form of fatigue crack growth rate as a basic parameter were Paris and co-workers [5].

$$\Delta K = K_{max} - K_{min} = Y(\sigma_{max} - \sigma_{min})(\pi a)^{1/2} = Y\Delta\sigma(\pi a)^{1/2} \tag{1}$$

The crack growth rates *da/dN* as a function of ΔK are determined from the corresponding curve a-N, graphically, or numerically. The experimental results presented on the double-logarithmic scale usually have a characteristic S-shape, schematically shown in **Figure 6**.

It is noticeable that the crack propagation is initially accelerated (area I), then passes into the phase of stable growth (area II), to finally pass into the phase of critical crack expansion (area III).

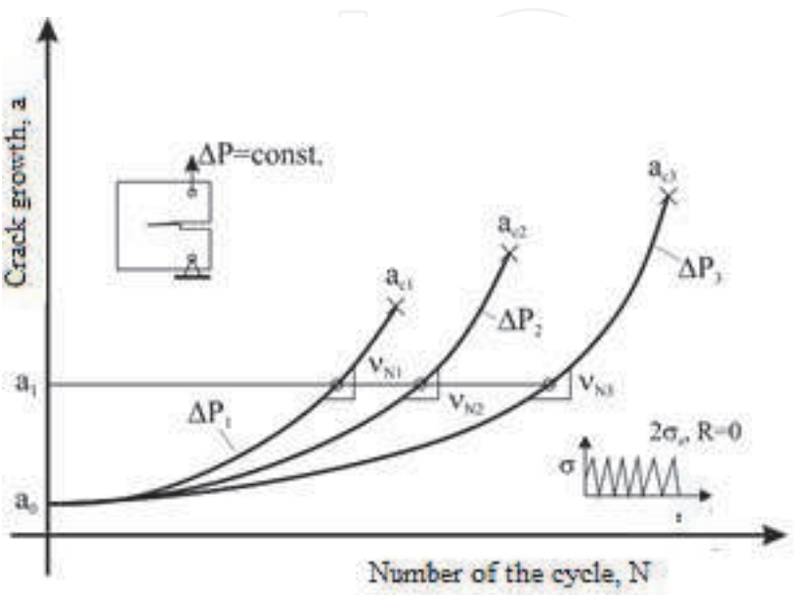

Figure 5.
Crack growth dependence a = f(N) for three levels of load ranges ΔP = const where ΔP1 < ΔP2 < ΔP3.

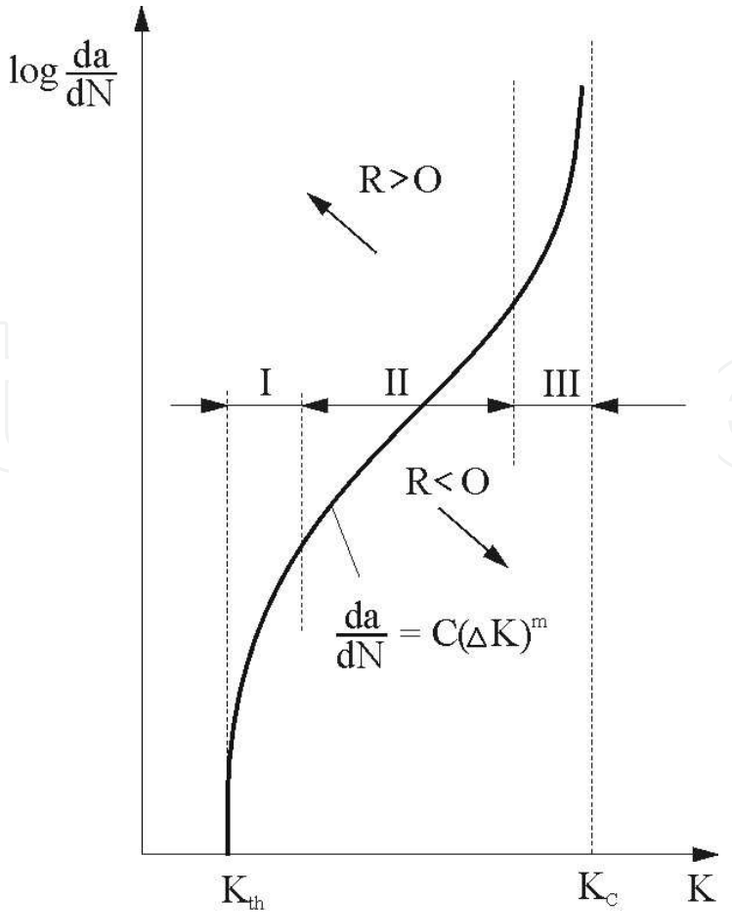

Figure 6.
The principle form of change of growth rate da/dN = f(ΔK) for R = and directions of displacement of S-curve for relations R≠o.

From the point of view of the crack growth mechanism and different intensities of influencing factors, three areas can be observed on this curve [6–8].

In area I, the crack propagation velocity tends to zero as the range of stress intensity factors approaches the crack propagation threshold:

$$\Delta K_{th} = K_{th,\max} - K_{th,\min} = \Delta\sigma\sqrt{\pi \cdot a_{th}} \cdot Y \tag{2}$$

where: a_{th}- the length of the initial crack.

In area II the crack grows linearly in the log–log diagram, so it can be described by the equation:

$$\frac{da}{dN} = C \cdot \Delta K^m \tag{3}$$

where C and m are the material constants determined experimentally.

This law is known as Paris' law.

In area III, the crack grows rapidly as the range of stress intensity factors approaches ΔK_c:

$$\Delta K_c = K_{Ic} - K_{c,\min} = \Delta\sigma\sqrt{\pi \cdot a_c} \cdot Y \tag{4}$$

where a_c - critical crack length, K_{Ic} - fracture toughness.

As Paris' law is valid only in area II, attempts were made to find equations that would describe crack growth in other areas of growth as well. One such is the Forman equation describing crack growth in areas II and III:

$$\frac{da}{dN} = \frac{C \cdot \Delta K^m}{(1-R) \cdot K_{Ic} - \Delta K} \tag{5}$$

Klesnil and Lucas modified the Paris law, taking into account the crack propagation threshold, and thus obtained the crack growth equation valid in areas I and II:

$$\frac{da}{dN} = C \cdot \left(\Delta K^m - \Delta K_{th}^m\right) \tag{6}$$

McEvily developed an expression that is valid for the whole crack growth curve, and which, unlike the previous equations, which were obtained empirically, is based on a simple physical model:

$$\frac{da}{dN} = C \cdot (\Delta K - \Delta K_{th})^2 \left(1 + \frac{\Delta K}{K_{Ic} - K_{\max}}\right) \tag{7}$$

From all these Eqs. (4), (5), (6) and (7) integration can obtain the time required for crack growth from any arbitrary to a critical length. Also, all the above terms are valid in the case of type i loads.

3.2 Determination of fatigue crack growth parameters

The basic progress that fracture mechanics has made in the sphere of material fatigue is in the analytical breakdown of the fatigue fracture phenomenon into the period of creation, in which the fatigue crack occurs, and the period of growth or expansion that follows and in which the resulting crack increases to a critical size at which a sudden fracture occurs. Thus, the total number of cycles, N_u, after which a fracture occurs, is divided by the number of cycles required for the fatigue crack to form, N_i, and the number of cycles for it to increase to the critical value for fracture, N_p, i.e., $N_u = N_i + N_p$, **Figure 7** [5].

Analysis of the stress state and deformation at the top of a rising fatigue crack by linear elastic fracture mechanics (LEFM) led to the formulation of the Paris equation for all metals and alloys, which relates the fatigue crack growth rate to the stress intensity range at the crack tip:

Although the Paris cracks growth equation is not valid in the whole range, between low velocities near the fatigue threshold ΔK_{th}, and high velocities K_{Ic}, the large linear midpoint of the curve covered by the Paris relation proved to be by far the most important from a practical point of view and fatigue crack growth.

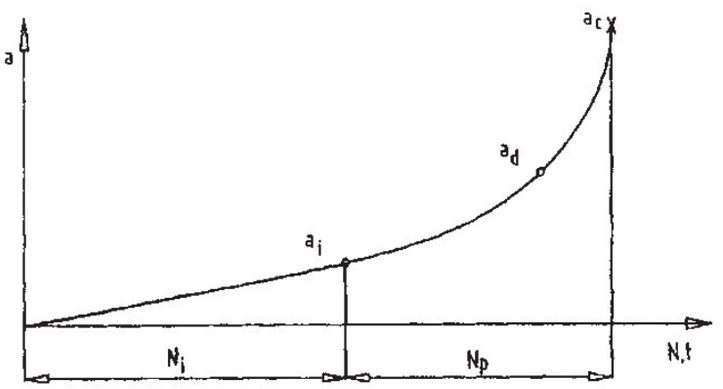

Figure 7.
The share of the initiation period N_i and the fatigue crack growth period N_p in the total fatigue life N_u.

The application of the Paris equation has proved particularly fruitful in the field of fatigue of structures made of high and very-high strength materials.

The ASTM E647 standard [9] prescribes the measurement of the fatigue crack growth rate da/dN, which develops from an existing crack, and the calculation of the stress intensity factor range, ΔK. This means that the test tube should have a tiring crack. There are two important limitations in the ASTM E647 standard: the growth rate must be greater than 10–8 m/cycle to avoid the fatigue threshold area, ΔKth, and the load should be of constant amplitude [4].

Steel of quality A-387 Gr was used to determine the dependence of the fatigue crack growth rate per cycle da/dN and the range of stress intensity factors ΔK. 91 15 mm thick [10]. The chemical composition and mechanical properties of the base material are given in **Tables 1** and **2**.

The welded joint is made with two welding processes and two additional materials.

- Root welding - TIG welding, additional material is wire marked BOEHLER C 9 MV-IG, diameter 2,4 mm (international designation W CrMo 91 according to EN ISO 21952-A).

- Filling - REL welding, additional material is an electrode marked BOEHLER FOX C9 MV, diameter 3,50 and 4,00 mm (international designation E CrMo 91 B 4 2 H5 according to EN ISO 3580-A).

Determination of fatigue crack growth rate da/dN and fatigue threshold ΔK_{th} was performed on standard Charpy tubes by the method of bending the tube at three points on a resonant high-frequency pulsator.

The test was performed at the same minimum and maximum load ratio R = −1. The achieved frequency ranged from 175 to 195 Hz depending on whether the crack passed through the base metal, weld metal, or the heat-affected zone, and on the magnitude of the load. The medium load and its amplitude were registered with accuracy ±3 Ncm.

Prior to the test, the specimen were mechanically prepared and measuring tapes - foils were glued to the prepared tubes, with which the crack growth was monitored. RMF A-5 measuring foils with a measuring length of 5 mm were used for testing. In order to be able to monitor the crack growth using a measuring foil, the FRACTOMAT crack growth detection device was used, **Figure 8**.

Chemical composition, mas. %										
C	**Si**	**Mn**	**P**	**S**	**Cr**	**Mo**	**Ni**	**V**	**Nb**	**Cu**
0.129	0.277	0.443	0.001	0.001	8.25	0.874	0.01	0.198	0.056	0.068

Table 1.
Chemical composition of the tested batch of steel SA 387 Gr. 91.

Yield strength R_{p02} **[MPa]**	**Tensile strength** R_m **[MPa]**	**Elongation A [%]**	**Impact energy Kv [J] +20°C**
445	580–760	18	40

Table 2.
Mechanical properties of the base material.

Figure 8.
Modern system for dynamic tests [10].

The scheme of the measuring foil and the method of registering crack growth is shown in **Figure 9**.

The appearance of the prepared specimen for determining the fatigue crack growth parameters is given in **Figure 10**.

Determining the dependence of the fatigue crack growth rate on the cycle da/dN and the range of stress intensity factors ΔK is reduced to determining the coefficient **C** and the exponent **m** in the Paris equation. The fatigue crack growth rate should be attributed to the current crack length, and, to the range of stress intensity factor, ΔK, which depends on the specimen geometry and crack length, and to the variable force range, $\Delta F = F_g - F_d$.

Determining the stress intensity factor range uses the formula

$$\Delta K = \frac{\Delta F \cdot L}{B\sqrt{W^3}} \cdot f(a/W) \tag{8}$$

where: L - range of supports, mm;
B - specimen thickness, mm;
W - width (height) of the specimen, mm, and.
a - crack length.

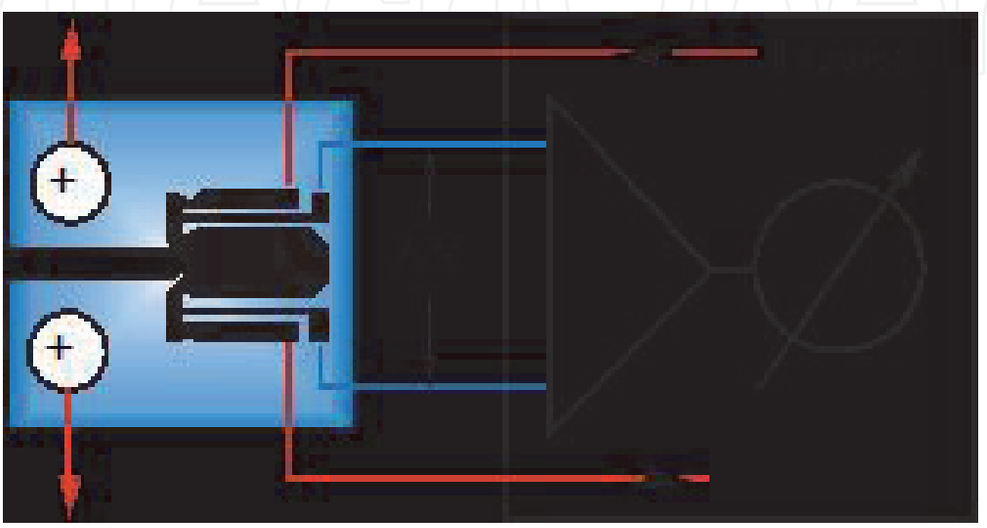

Figure 9.
The scheme of the measuring foil and the method of registering crack growth.

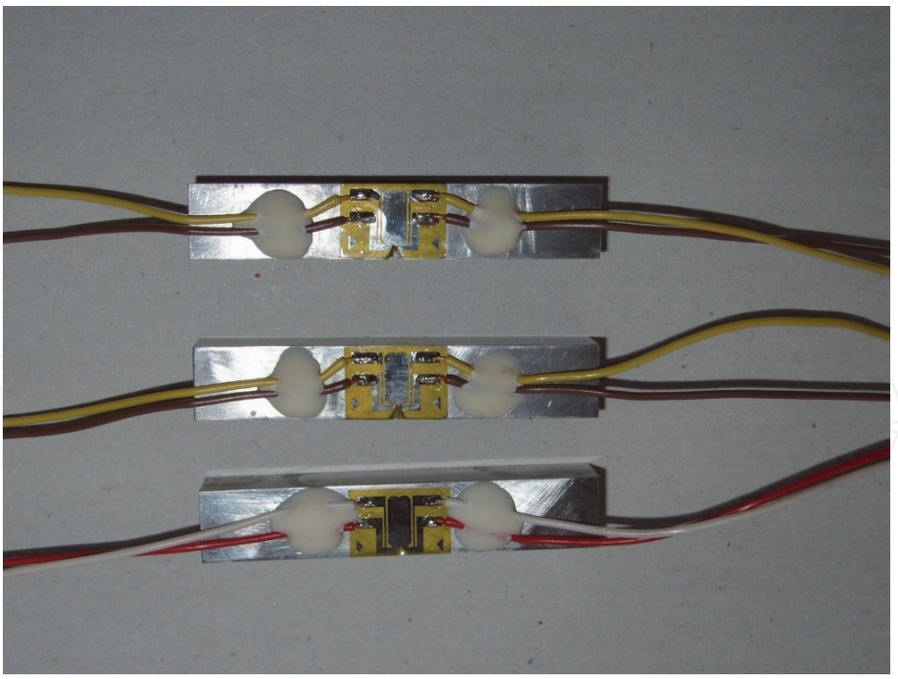

Figure 10.
The appearance of the prepared specimen for parameter testing [10].

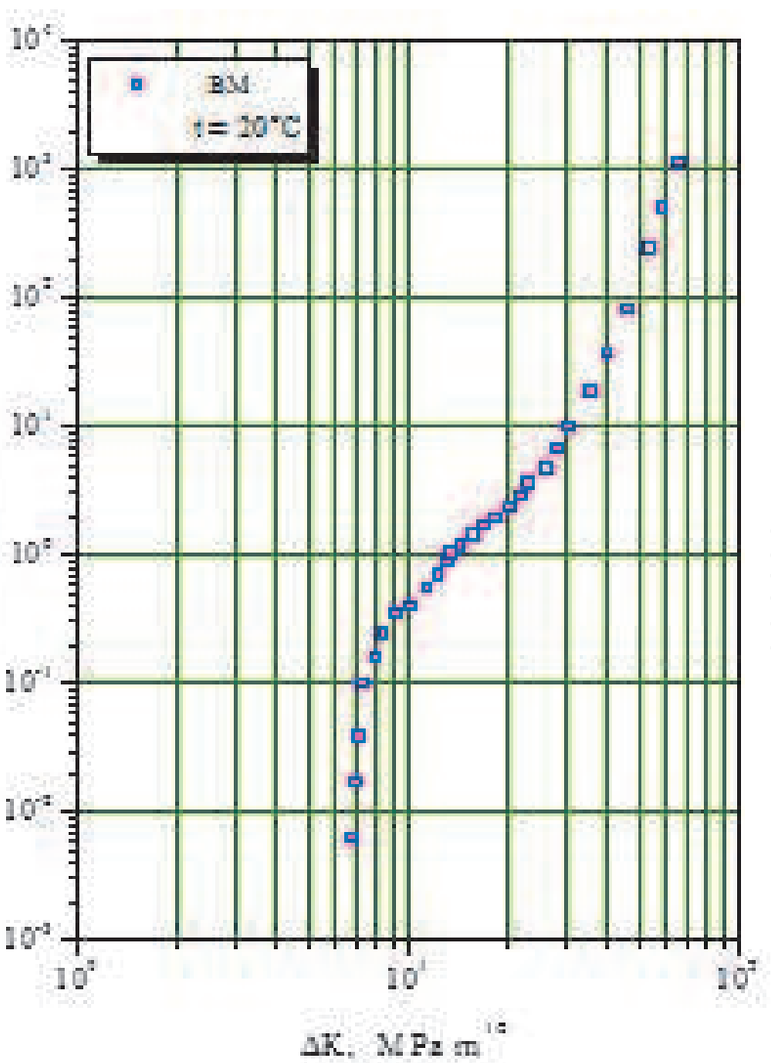

Figure 11.
Dependence diagram da/dN - ΔK for specimens with fatigue crack tip in BM [10].

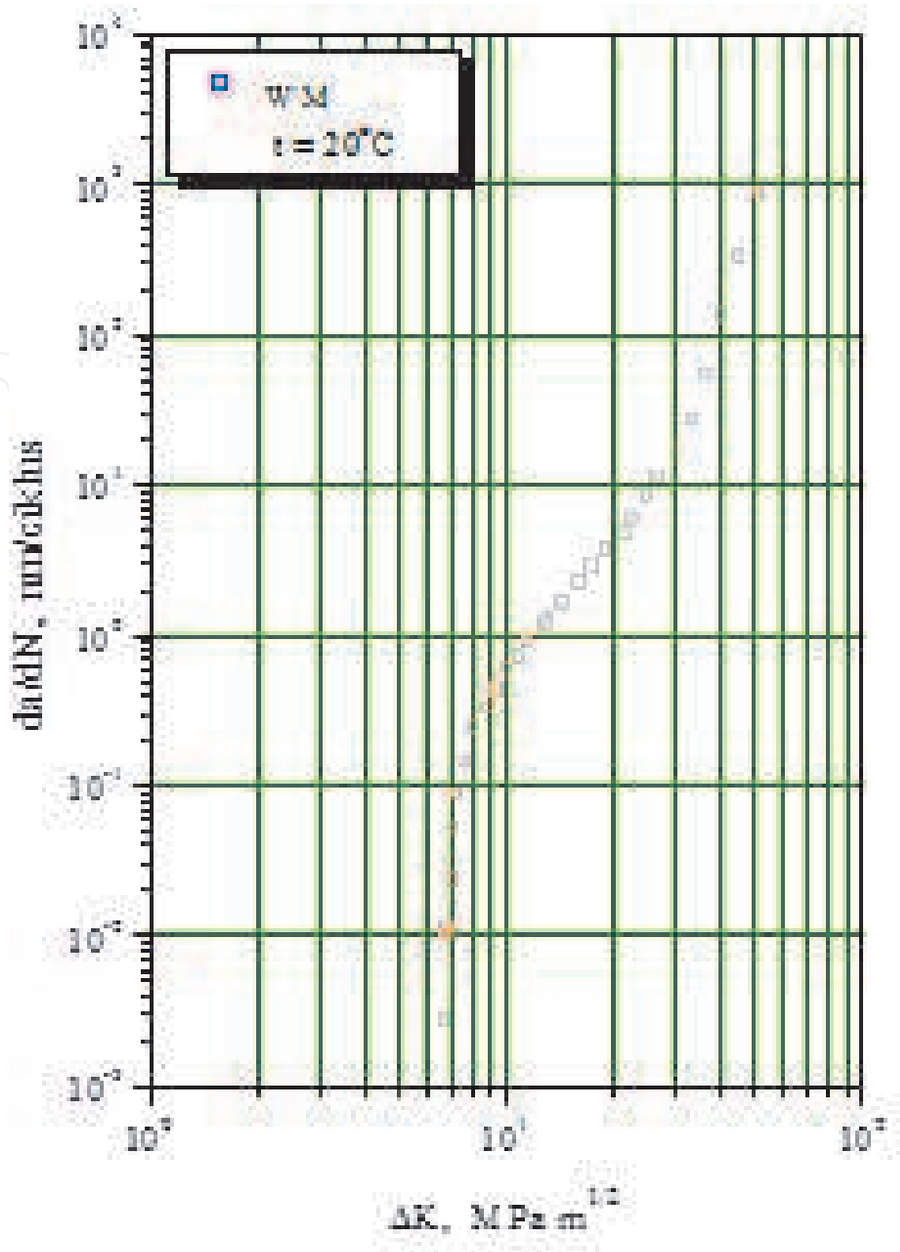

Figure 12.
Dependence diagram da/dN - ΔK for speciemens with fatigue crack tip in WM [10].

The geometric term f (a/W) is given by the expression:

$$f(a/W) = \frac{3 \cdot \sqrt{\frac{a}{W}} \cdot \left[1,99 - \frac{a}{W}\left(1 - \frac{a}{W}\right)\left(2,15 - 3,93\frac{a}{W} + 2,7\left(\frac{a}{W}\right)^2\right)\right]}{2\left(1 + 2\frac{a}{W}\right)\left(1 - \frac{a}{W}\right)^{3/2}} \qquad (9)$$

Three groups of specimens depending on the location of the crack tip were examined, namely:

Group I - specimens with a crack tip in BM,

Group II - specimens with a crack tip in WM and.

Group III - specimens with a crack tip in HAZ.

Based on the test flow and the obtained dependences of crack length **a** - number of cycles **N**, the fatigue crack growth rate da/dN is calculated. Depending on the applied variable load expressed through the change of the range of voltage intensity factor, ΔK, log da/dN - log(ΔK) curves are drawn.

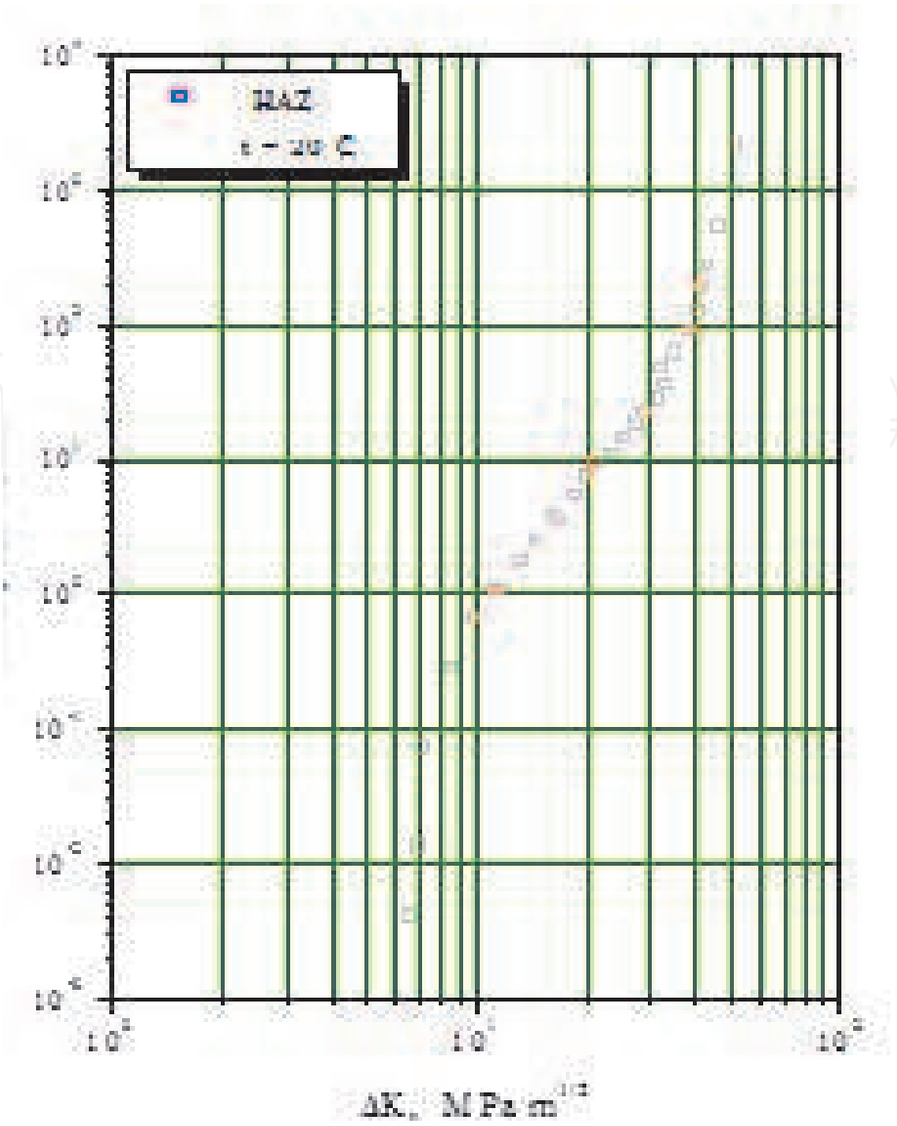

Figure 13.
Dependence diagram da/dN - Δ for specimens with a fatigue crack tip in HAZ [10].

Characteristic diagrams of fatigue crack growth rates, da/dN - change of stress intensity factor range, ΔK, for specimens with fatigue crack tip in BM, **Figure 11**., for specimens with fatigue crack tip in WM, **Figure 12**., and for specimens with a fatigue crack tip in HAZ, **Figure 13**.

The obtained values of the parameters of the Paris equation, coefficient C and exponent m, fatigue threshold ΔK_{th}, and fatigue crack growth rate, da/dN, at the value of ΔK = 10 MPa $m^{1/2}$, are given in **Table 3** for specimens with a notch in BM, **Table 4** for specimens with a notch in WM, and **Table 5** for speciemns with a notch in HAZ.

Test tube label	Test temperature, °C	Fatigue threshold ΔK_{th}, MPa $m^{1/2}$	Coefficient C	Exponentm	da/dN, µm/cikl, pri ΔK = 10 MPa $m^{1/2}$
OM-1	20	6,9	$2{,}98 \cdot 10^{-10}$	3,62	$1{,}24 \cdot 10^{-6}$
OM-2		6,8	$3{,}07 \cdot 10^{-10}$	3,58	$1{,}17 \cdot 10^{-6}$
OM-3		7,1	$2{,}85 \cdot 10^{-10}$	3,59	$1{,}11 \cdot 10^{-6}$

Table 3.
Fatigue crack growth parameters for notched specimens in BM.

Test tube label	Test temperature, °C	Fatigue threshold ΔK_{th}, MPa $m^{1/2}$	Coefficient C	Exponentm	da/dN, µm/cikl, pri ΔK = 10 MPa $m^{1/2}$
MŠ-1	20	7,2	$3,88 \cdot 10^{-10}$	3,62	$2,56 \cdot 10^{-6}$
MŠ-2		7,1	$4,05 \cdot 10^{-10}$	3,71	$2,07 \cdot 10^{-6}$
MŠ-3		7,4	$3,93 \cdot 10^{-10}$	3,80	$2,48 \cdot 10^{-6}$

Table 4.
Fatigue crack growth parameters for notched specimens in WM.

Test tube label	Test temperature, °C	Fatigue threshold ΔK_{th}, MPa $m^{1/2}$	Coefficient C	Exponentm	da/dN, m/cikl, pri ΔK = 10 MPa $m^{1/2}$
ZUT-1	20	6,6	$3,05 \cdot 10^{-10}$	4,01	$3,12 \cdot 10^{-6}$
ZUT-2		6,8	$3,07 \cdot 10^{-10}$	4,04	$3,37 \cdot 10^{-6}$
ZUT-3		6,5	$2,85 \cdot 10^{-10}$	4,09	$3,51 \cdot 10^{-6}$

Table 5.
Fatigue crack growth parameters for notched specimens in HAZ.

4. Conclusions

Practice has shown that structures that are exposed to the effects of variable load during operation are most prone to accidents and fractures. The causes are primarily errors that occur in exploitation.

- The reason for the application of fracture mechanics is based on the fact that in the presence of errors, which inevitably occur as a result of imperfections in production processes and/or in operation, there is a loss of load-bearing structure elements and time as a whole.

- The reduction of load-bearing capacity in order to achieve the reliability and safety of structures must be controlled.

- The obtained values of the fatigue threshold ΔKth represent important data on the quality of the tested materials from the aspect of its micromechanical properties, ie on the behavior in the presence of cracks. After its determination, the magnitudes and periods of action of the variable load are known for the formation and then for the growth of the tired crack until cracking.

Author details

Mersida Manjgo[1*] and Meri Burzic[2]

1 Džemal Bijedić University, Faculty of Mechanical Engineering, Mostar, Bosnia and Herzegovina

2 University of Belgrade, Innovation Center, Faculty of Mechanical Engineering, Belgrade, Serbia

*Address all correspondence to: mersida.manjgo@unmo.ba

References

[1] Fuchs H. O., Stephens R. I. Metal Fatigue in Engineering. A Wiley-Intersciene Publication. New York: John Wiley and Sons; 1980.

[2] Podrug S. Mehanika loma. Split: Fakultet elektrotehnike, strojarstva i brodogradnje; 2009.

[3] ASTM E466–82. Standard Practice for Conducting Constant Amplitude Axial Fatigue Test of Metalic Materials. Annual Book of ASTM Standard; 1986.

[4] M. Manjgo, Kriterijumi prihvatljivosti prslina u zavarenim spojevima posuda pod pritiskom od mikrolegiranih čelika, Doktorska disertacija, 2008

[5] V. Ćulafić, Uvod u mehaniku loma, Podgorica

[6] Heckel K. Einfuhrung in die technische Anwendung der Bruchmechanik. Munchen: Carl Hanser Verlag; 1970.

[7] Ekberg A. Fatigue crack propagation. Gothenborg: Chalmers Solid Mechanics; 2003.

[8] Ritchie R. O. Mechanisms of fatigue-crack propagation in ductile and brittle solids. Netherlands: International Journal of Fracture 100: 55–83, 1999.

[9] ASTM 647 Standard Test Method for Constant-Load-Amplitude Fatigue Crack Growth

[10] M. Manjgo, M. Burzić, Optimal welding parameters of SA 387 Gr. 91 thick steel plates in corrosive environment, Elobarat po projektu Eureka, Beograd-Mostar, 2016–2019.